LA-UR- 09-00062

Approved for public release;
distribution is unlimited.

Title:	Direct Measurement of the alpha-epsilon Transition Stress and Kinetics for Shocked Iron
Author(s):	B.J. Jensen G.T. Gray III R.S. Hixson
Intended for:	Publication in the Journal of Applied Physics

Form 836 (7/06)

Direct Measurements of the α-ϵ Transition Stress and Kinetics for Shocked Iron

B.J. Jensen,* G.T. Gray III, and R. S. Hixson†
Los Alamos National Laboratory, Los Alamos NM 87545

Iron undergoes a polymorphic phase transformation from alpha phase (bcc) to the epsilon phase (hcp) when compressed to stresses exceeding 13 GPa. Because the epsilon phase is denser than the alpha phase, a single shock wave is unstable and breaks up into an elastic wave, a plastic wave, and a phase transition wave. Examination of this structured wave coupled with various phase transformation models has been used to indirectly examine the transition kinetics. Recently, multimillion atom simulations (molecular dynamics) have been used to examine the shock-induced transition in single crystal iron illustrating an orientation dependence of the transition stress, mechanisms, and kinetics. The objective of the current work was to perform plate impact experiments to examine the shock-response of polycrystalline and single crystal iron with nanosecond resolution for impact stresses spanning the $\alpha - \epsilon$ transition. The current data reveal an orientation dependence of the transition stress coupled with a transition time that is nonlinearly dependent on the impact stress with a duration ranging from picoseconds to hundreds of nanoseconds. The higher transition stress for iron[100] is in agreement with the predictions from MD calculations that describe an orientation dependence of the transition stress. However, MD calculations do not capture the complexity of the continuum states achieved or the transition kinetics. Further results and implications are discussed in this paper.

I. INTRODUCTION

The dynamic response of polycrystalline iron has been studied extensively over the last fifty years due to its importance in industry as well as its role in the earth's core. Dynamic experiments began in the 1950s with Bancrofts[1] shock wave experiments on Armco iron where a three wave structure was observed consisting of an elastic wave, a P1 wave (plastic wave), and a P2 wave (phase transforming wave) for impact stresses greater than 13 GPa indicative of a polymorphic phase transformation. Subsequent experimental work using x-ray diffraction methods[2,3] provided evidence that polycrystalline iron transformed from the alpha (bcc) phase to the epsilon (hcp) phase when compressed above 13 GPa. Barker and Hollenbach[4] used a velocity interferometer (VISAR) to obtain particle velocity records for shocked iron providing valuable information regarding the elastic limit of iron and the transformation kinetics. In 1973, Andrews[5] developed a thermodynamically consistent equation of state to describe the shock wave propagation of polycrystalline iron undergoing a phase transformation. Theoretical efforts were continued by Boettger and Wallace[6] with the development of a continuum model that incorporated metastability (for the α-ϵ transition) where the transition kinetics were described by a linear function with respect to impact stress that was obtained by analyzing previous wave profile data for iron.

More recently, efforts have focused on investigating the phase transition in defect-free iron single crystals using multimillion-atom molecular dynamics simulations.[8,9] Results from these calculations demonstrated an orientation dependence of the transition stress, mechanisms, kinetics, and Hugoniot response. Specifically, for the [100] orientation, it was found that the transition stress was higher than the experimentally determined polycrystal value of 13 GPa by approximately 2 GPa. Furthermore, the transition time was found to be very fast (approximately 50 ps) due to the martensitic nature of the transition with shuffle (not shear) being the dominant mechanism. These calculations have provided a wealth of information that has not been fully examined experimentally due to the lack of measurements that directly examine the phase transition and the associated kinetics, at the atomic and continuum length scales, in single crystal iron. Preliminary wave profile data have been reported[10] for shocked and ramp-loaded iron single crys-

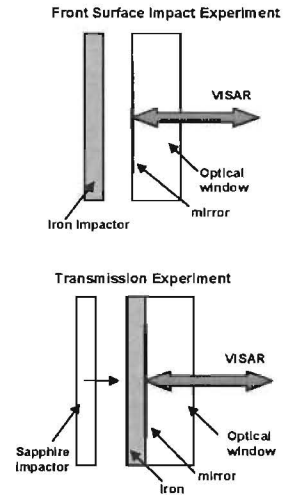

FIG. 1: Experimental configuration for front-surface and transmission plate impact experiments. An interferometric method (VISAR) was used to obtain the particle velocity history at the iron/sapphire interface.

TABLE I: Relevant experimental parameters and calculated quantities

Shot #	Vp (km/s) (±0.1%)	Sample	L (mm) (±1.5μm)	Peak State u_p^m (km/s) (±0.5%)	Peak State u_p (km/s) (±0.6%)	Peak State P_x (GPa) (±0.5%)	Peak State U_s (km/s) (±0.9%)	Overshoot u_p^m (km/s) (±0.5%)	Overshoot u_p (km/s) (±0.6%)	Overshoot P_x (GPa) (±0.5%)	Overshoot U_s (km/s) (±0.9%)	ΔP (kbar)	T (μs)
56-05-25	0.767	Poly	1.000	0.381	0.385*	18.03*	–	–	–	–	–	–	–
56-05-22	0.725	[100]	0.708	0.385	–	–	–	–	–	–	–	–	–
56-05-42	0.784	[100]	0.613	0.342	0.439	15.86	4.596	0.373	0.411	17.19	5.320	29.3	0.015
56-05-43	0.707	[100]	0.635	0.321	0.389	14.58	4.867	0.334	0.373	15.34	5.232	10.8	0.092
56-05-44	0.682	[100]	0.307	0.315	0.367	14.44	5.006	0.322	0.360	14.77	5.220	5.10	0.120
56-05-32	0.757	Poly	1.000	0.330	0.427	15.15	4.465	0.361	0.396	16.62	5.300	37.3	0.020
56-06-02	0.546	[100]	0.336	0.258	0.288	11.77	5.199	–	–	–	–	–	–
56-06-03	0.621	[100]	0.354	0.293	0.320	13.36	5.200	–	–	–	–	–	–
56-08-05	0.695	Poly	0.655	0.307	0.388	14.04	4.604	0.328	0.367	15.05	5.226	21.6	0.120
56-08-06	0.709	Poly	2.098	0.313	0.396	14.35	4.609	0.3355	0.374	15.41	5.249	25.2	0.077
69-08-16	1.250	[100]	0.385	0.448	0.577	20.78	4.581	–	–	–	–	65.2	<0.001
56-08-53	0.676	Poly	3.542	0.303	0.396	13.88	4.609	0.3165	0.3595	14.51	5.136	16.2	0.200

*Values obtained from a wave code calculation that used a phase transition model for polcrystal iron[7]

tals that exhibited the typical three wave structure. In addition, x-ray diffraction experiments were performed on shock-compressed (Laser-driven shock) single crystal iron[11] where it was verified that the lattice transforms from the bcc to the hcp phase during dynamic loading. These results provided important information on the atomic structure for iron shocked through the phase transition, but the x-ray diffraction data were not sufficiently correlated to the continuum state of the material because the experiments were time-integrated and simultaneous continuum measurements were not performed as has been done in past work on LiF.[12]

The objectives of the current work were to obtain direct measurements of the transition stress, kinetic rates, and the metastable Hugoniot equations for shocked polycrystal iron and single crystal iron oriented along the [100] direction. These objectives were addressed by performing front-surface plate impact experiments[13] using VISAR[14] to obtain particle velocity histories for iron in the 50-180 kbar range spanning the α to ϵ transition. The results are compared to current predictions obtained from the molecular dynamics simulations of single crystal iron and past work on polycrystalline iron.

II. EXPERIMENTAL METHODS

Front-surface plate impact experiments were performed on high-purity iron single and polycrystalline iron samples using a 50 mm gas-gun. The experimental configuration is shown in Fig. 1 and consisted of an iron sample backed by foam impacting an aluminum plated sapphire window (z-cut). Unlike previously reported plate impact experiments which used model calculations to infer the transition kinetics, the front surface configuration eliminates complications due to wave interactions and wave propagation by directing the structured shock wave back into the projectile away from the measurement interface.[13] Thus, the transition kinetics can be observed directly by monitoring the particle velocity (or stress) history at the sample/window interface. Particle velocity profiles were obtained at the iron/sapphire interface using the standard push-pull[15] VISAR system with a time resolution of approximately 1 ns. The wave profile data combined with the measured projectile velocity and the known shock response for the sapphire crystals[16–18] provided the data needed to determine the stress history at the interface. In addition to front surface experiments, two transmission experiments were performed to examine the shock wave profile for a thick crystal for characterization and comparison with past work. The experimental configuration is shown in Fig. 1 and consisted of a sapphire crystal impacting an iron/sapphire target.

Projectile velocities were measured using a standard shorting pin method.[16] A total of eleven shorting pins (one pin served as the ground pin) were placed at 30° increments on a 1.25-inch radius about the center of the barrel with the pin heights placed at random heights above the target from 1-12 mm. As the projectile impacted each pin, electrical signals were generated, separated in time due to the different heights, and recorded on a digitizer. These signals were used to calculate both the velocity and the tilt of the projectile during impact. Velocity uncertainties from the shorting pins are approximately 0.1% in the velocity range of 0.3 to 1 km/s.

All experiments were performed on high-purity single crystal iron (99.94 % purity) oriented along the [100] directions. The [100] iron samples were cut from the boule (originally oriented along the [210] direction), oriented using Laue backscatter diffraction, using a precision low-speed diamond saw to the desired thickness. The crystals were lapped flat and to the desired thicknesses and were made parallel within 1-3 microns over the 10-mm diameter. To provide a comparison with the single crystal data, experiments was also performed using a polycrystalline ARMCO iron sample similar to sam-

ples used in past work[7].The VISAR optical windows were well-characterized, high-purity Hemlux grade z-cut sapphire samples obtained from Crystal Systems. Sapphire was chosen as the optical window for this work because of the well-characterized optical[16,19,20] and shock wave properties[18] and because sapphire remains elastic within the stress range of interest. All windows were chemically polished on both sides and were flat and parallel to 0.0002", and oriented within ±15'. The nominal thickness and density of the windows were 19mm and 3.985 g/cc, respectively.

III. EXPERIMENTAL RESULTS

A total of ten front-surface impact and two transmission experiments were performed on iron in this work. The relevant experimental parameters, measured quantities, and calculated quantities are presented in Table I. The measured projectile velocity (V_p), sample orientation, and sample thickness (L) are shown in columns two through four, respectively. The measured particle velocities (u_p^m) for the peak steady state are given in column five. These values were used to calculate the particle velocity along the iron Hugoniot given in column six (u_p) by subtracting the measured particle velocity from the projectile velocity. The Hugoniot data point is completed by determining the longitudinal stress (P_x) from the known Hugoniot for the sapphire windows (column seven). The values for the shock velocity (U_s) were obtained using the Rankine-Hugoniot jump conditions[21] and these values are shown in column eight. A similar procedure was followed to calculate the Hugoniot data point for the transient state, observed as an overshoot in the particle velocity data. These values are listed in columns nine through twelve. The change in stress ΔP defined as the difference between the impact stress (Table I, column 11) and the transition stress (Table II) is shown in column thirteen and the measured transition times for the α-ϵ transition in column fourteen.

Two transmission experiments (Shot #56-05-25 and #56-05-22) were performed to characterize the samples used in this work by examining the shock wave profile and measure the elastic wave amplitude. The projectile velocities were 0.767 (polycrystal) and 0.725 km/s (single crystal) which translates to a peak stress of 17.5 GPa for the polycrystal sample. Both experiments used sapphire impactors and sapphire optical windows with nominal thickness of 3 mm and 19 mm, respectively. The resulting wave profiles are shown in Fig. 2 where the particle velocity (km/s) is plotted versus time (μs). The wave profiles were comparable to those reported in past work[4] where a three wave structure was observed consisting of an elastic wave, a plastic wave (or P-I wave), and a phase transition wave (P-II wave). The wave profiles are seen to be remarkably similar with comparable peak particle velocity state and comparable arrival times for the P-II wave. This latter observation suggests that the transition

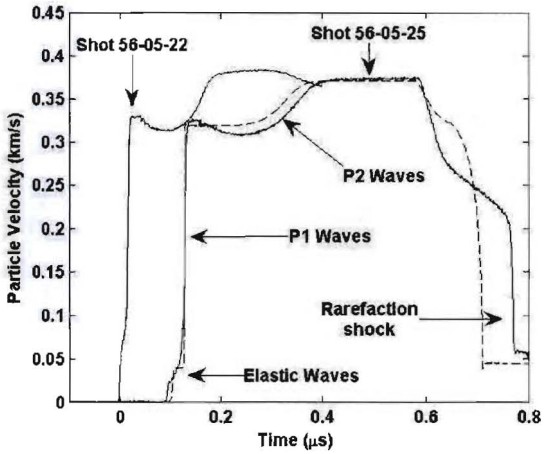

FIG. 2: Wave profiles obtained from the transmission experiments for single crystal iron (Shot #56-05-22) shocked along the [100] direction and polycrystalline iron (Shot #56-05-25). The dashed line is a calculation using the Andrews EOS[5] for polycrystalline iron.

time for the [100] sample is comparable to the polycrystal samples contrary to MD calculations[9] that predict a subnanosecond transition time. Following the peak steady state, the polycrystal wave profile exhibits the typical rarefaction shock due to the impactor release. This was not observed in the single crystal sample because edge waves, due to the small 10-mm diameter samples, terminated the experiment before the release could reach the measurement interface.

Wave profiles from three of the front-surface impact experiments are shown in Fig. 3 where the particle velocity (km/s) of the interface is plotted versus time (μs). In contrast to previous wave profiles[4,10] obtained for iron which exhibited a three-wave structure, the wave profiles shown in Fig. 3 exhibit a sharp jump in velocity followed by either a steady state or relaxation to a steady state. In the following analysis, it will be shown that the initial spike represents the initial instantaneous (or metastable) compression along the α-phase (Phase I) Hugoniot while the relaxation characterizes the transition to the ϵ-phase (Phase II) Hugoniot. In addition to the initial shock compression, the impactor release due to wave reflection from the back surface of the iron impactor was observed. For the higher velocity experiments, the typical rarefaction shock is observed due to phase reversion (ϵ to α) indicating that the impact stress achieved was sufficient to induce the initial phase transition. For the low velocity experiment where the impact stress is expected to be below the phase transition stress, an elastic-plastic release is observed. Three additional experiments (56-05-32, 56-08-05, and 56-08-06) were front-surface experiments using polycrystal ARMCO iron to provide additional data in the vicinity of the phase transition for a more direct

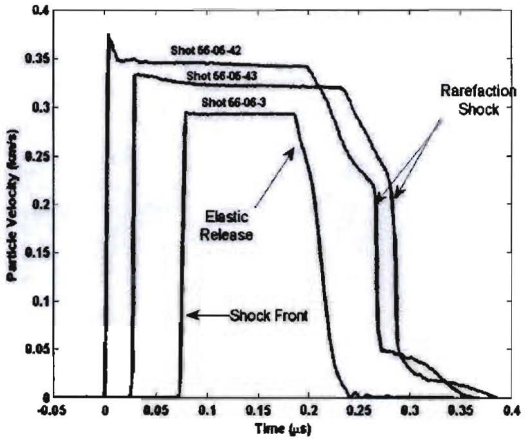

FIG. 3: Wave profiles obtained from the front-surface impact experiments for single crystal iron shocked along the [100] direction. For impact stresses greater than the transition stress, a spike is observed followed by relaxation to a steady state. Below the transition stress, a square wave is observed followed by the typical elastic-plastic release.

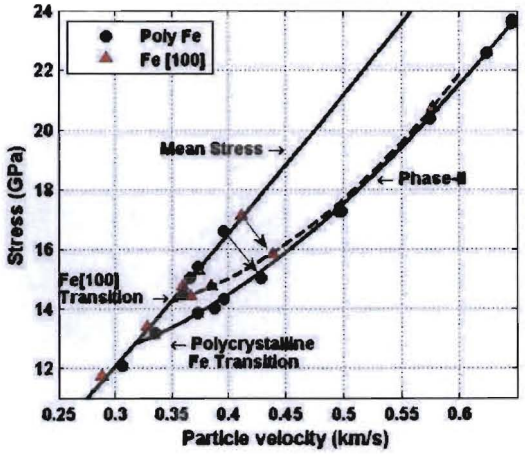

FIG. 4: Plot of longitudinal stress versus the measured particle velocity for single crystal and polycrystalline iron experiments. The dashed curves represent the Hugoniot equations given by the polynomials $P_x^{100} = 19.69 - 41.98u_p + 75.31u_p^2$ and $P_x^{poly} = 16.3 - 40.4u_p + 105u_p^2 - 38.6u_p^3$.

comparison with the single crystal data. The data are summarized in Table I. The particle velocity histories obtained exhibited similar features to the single crystal data.

IV. ANALYSIS

The data analysis for the iron experiments is presented in this section. First, the elastic longitudinal stress, shock velocity, and mean stress are calculated using the available elastic constants. Second, the data are plotted to determine the Hugoniot equations for both polycrystalline iron and single crystal iron near the phase transition. These equations are then used to determine the transition stress for the α-ϵ transition. Subsequently, wave profile data are used to directly determine the transition time.

The analysis presented in this section requires the elastic longitudinal stress (P_x^e), the shock velocity (U_s), and the mean stress (P) for the single crystal iron samples as functions of particle velocity or density compression. These relations were calculated using the available second and third-order elastic constants[22,23] and the nonlinear elastic equations[24] which relate the stress to the density compression and the particle velocity. The nonlinear-elastic equations for the longitudinal (P_x^e)and transverse stress (P_y^e)are:

$$P_x^e = c_{11}e - (\frac{3c_{11}}{2} + \frac{c_{111}}{2})e^2 \quad (1)$$

$$P_y^e = c_{12}e + (\frac{c_{12}}{2} - \frac{c_{112}}{2})e^2 \quad (2)$$

where c_{11}, c_{12} are the second order elastic constants, c_{111} and c_{112} are the third order elastic constants, and e is the strain defined in terms of the density compression e = $\mu/(1+\mu)$. Using the elastic constants $c_{11} = 231.0$ GPa, $c_{12} = 135.0$ GPa, $c_{44} = 110.86$ GPa, $c_{111} = -2800.0$ GPa, and $c_{112} = -800.0$ GPa, the equations for the longitudinal stress, the mean stress, and the shock velocity for iron[100] are:

$$P_x^e = 11.88u_p^2 + 43.67u_p \quad (3)$$

$$P = 10.44u_p^2 + 37.2u_p \quad (4)$$

$$U_s^e = 5.425 + 2.152u_p - 0.6803u_p^2 \quad (5)$$

where the stress values are in units of GPa and u_p is the particle velocity in units of km/s. The longitudinal stress (Equation 3) was used to determine the stress at the elastic wave front for the transmission experiment on single crystal iron. From the data, the elastic wave amplitude was determined to be 0.052 km/s. Using Equation 3 and the known Hugoniot for sapphire coupled with the standard impedance matching method, the stress of the elastic wave was 23.1 $\pm$ 0.5 kbar, respectively.

The experimental results are shown in Fig. 4 where the longitudinal stress is plotted versus the particle velocity. The black-filled markers represent the polycrystalline data available for iron[4] in the stress range of interest including the three experiments performed in this work. The red-filled triangles represent the single crystal iron data. For all data, the error bars (uncertainties are shown in Table I) lie well within the boundaries of each data-point marker. For comparison, the mean stress curve given by equation 4 which represents the phase-I (α) because it is in close agreement with the poly-

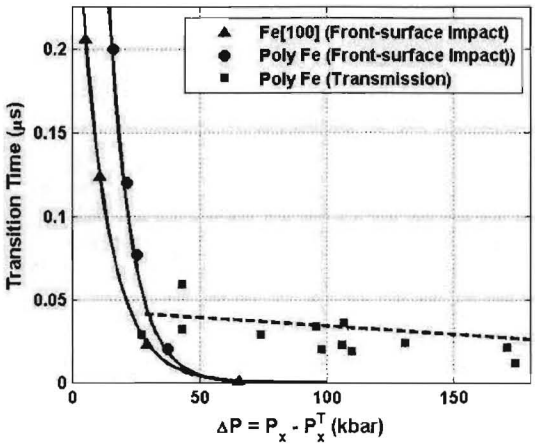

FIG. 5: Plot of the transition time versus ΔP determined from the front-surface impact experiments. The filled triangles and circles indicate the data obtained for the iron [100] single crystals and the polycrystalline iron, respectively. The filled squares represent the previous transition time estimates for transmission experiments.[6]

crystalline data and the previously reported metastable Hugoniot for ϵ-iron by Brown[25] (Us = 4.64 + 1.48 u_p) not shown in Fig. 4. The data in Fig. 4 show that for impact stresses below the phase transition, the peak stress state lies along the mean stress curve. Above a transition stress, a transient response is observed consistent first with compression along the mean stress curve followed by relaxation to a transformed Hugoniot as indicated by the arrow in Fig 4 for two of the experiments. Above approximately 18 GPa, the single crystal data lies along the polycrystalline Hugoniot. To determine the transition stress, the data shown in Fig. 4 were fit using second and third-order polynomials to determine the Hugoniots (see Fig 4). The intersection of the fit with with the α-phase Hugoniot was taken as the phase transition stress. For polycrystalline and single crystal iron the transition stress are 12.89±0.15 GPa and 14.26±0.14 GPa, respectively. Thus, the transition stress for polycrystalline iron is consistent with the values reported elsewhere whereas the single crystal value is 1.4 GPa greater than the polycrystal samples.

As shown in Fig. 4, for impact stresses greater than the transition stress,the iron crystals undergo a transition from the phase-I to the Phase II Hugoniot. In past work, the transition kinetics have been determined indirectly by analyzing wave profile data obtained from transmission experiments using a wave code that incorporated a phase transition model with a time constant to describe the transition.[4,6,7] In this work, the transition time can be estimated directly from the particle velocity data shown in Fig. 3. To determine the transition time, the particle velocity data were fit using an exponential function to describe the relaxing region of the wave profile and the transition time was taken as the value at the 95% level. The results are summarized in Table I (column 13) and in Fig. 5 where the change in longitudinal stress $\Delta P = P_x - P_x^T$(column 13) is plotted versus the measured transition times (column 14) for each experiment where P_x^T is the transition stress. The uncertainty in the values for ΔP were estimated to be approximately ±0.23 GPa based on the uncertainties given for the longitudinal stress and the transition stress. The single crystal and polycrystal iron data obtained from the front-surface experiments were found to be best described by the exponential functions

$$T^{100} = 0.33exp(-0.09\Delta P) \quad (6)$$

$$T^{poly} = 1.1exp(-0.11\Delta P) \quad (7)$$

with transition times T ranging from hundreds of nanosecond for impact stresses (near the transition) to subnanoseconds as the impact stresses approaches the 180-200 kbar range. This observation is consistent with the MD calculations[9] which predict a subnanosecond transition time for the [100] orientation of iron for impact velocity of approximately 1 km/s well within the over-driven regime. The polycrystal data obtained in this work show a similar response though the transition proceeded at a slower rate as compared to the single crystal data for a given impact stress. A high stress experiment was not performed for the polycrystal crystal data though the trend would suggest that the behavior is similar to the single crystal trend.

V. DISCUSSION

Transition kinetics have been examined in past work by Boettger and Wallace[6] where transmission wave profile data obtained by Barker[4] were analyzed to estimate the transition times from P2 wave rise time. The resulting data are shown plotted in Fig. 5 along with the transition time data obtained from the current work. These data exhibit significant scatter with a linear fit that extrapolates to an intercept of 40-50 ns, significantly less than the value found for the front surface experiments. Furthermore, the values approach a minimum transition rate of approximately 20-30 ns in contrast to the front-surface impact data that point toward a sub-nanosecond transition at high-impact stresses. As an independent check on this analysis method, the wave profile obtained from experiment 56-04-25 was compared to a wave profile calcu-

TABLE II: Experimental values at the phase transition

Measured/Calculated Parameters	Fe [100]	Polycrystal iron	Units
Particle velocity	0.350±0.003	0.318±0.003	(km/s)
Long. stress	14.26±.14	12.89±.15	(GPa)
Shock Velocity	5.188±0.100	5.143±0.100	(km/s)

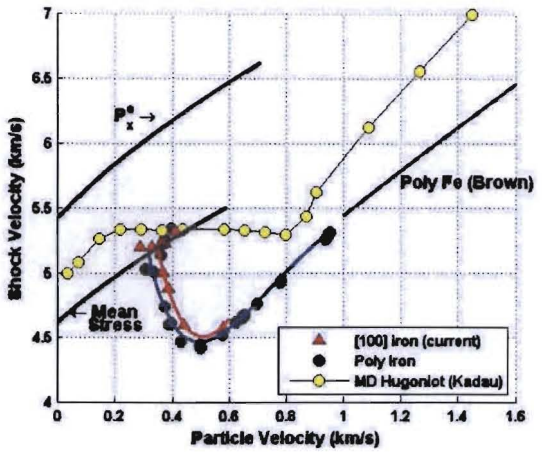

FIG. 6: Plot of the shock velocity (km/s) versus the particle velocity (km/s). The experimental data for polycrystal and single crystal iron data are shown along with various calculated curves including the results from molecular dynamics simulations.

lated using a one-dimensional wave code (WONDY) that incorporated a non-equilibrium phase transition model developed by Andrews[5] that was used in past work to analyze transmission data.[7] The calculated wave profile (with an estimated transition time of approximately 20 ns) is shown in Fig. 2 along with the experimental data. Although there are differences between the two wave profiles, the model sufficiently agrees at the peak state and at the P1 wave with a comparable rise time for the P2 wave providing additional data that illustrate the different response of iron obtained from the two experimental configurations. Based on these results, it is concluded that the transition rate and likely the transition mechanisms depend on the impact stress and the sample thickness.

Finally, it is useful to compare the Hugoniot data obtained in this work with the results from previous molecular dynamics simulations for iron shocked along the [100] direction.[9] The single crystal results for a calculation performed for an impact velocity of 1.087 km/s are shown in Fig. 6 where the shock velocity (km/s) is plotted versus the particle velocity (km/s). Also shown are the experimental data for polycrystal and single crystal iron and the calculated elastic compression curve, the mean stress curve, and the high-pressure iron Hugoniot obtained from past work[25]. The following observations were made: 1) the elastic response predicted by the MD simulations does not agree with the calculated elastic Hugoniot, but lies in between the elastic curve and the mean stress curve, 2) the transition to the ϵ -phase Hugoniot is represented as a nearly horizontal line that connects the elastic response to the ϵ -phase Hugoniot, and 3) The high-pressure Hugoniot does not agree with the experimental data. The reasons for the discrepancies have been discussed in detail by Kadau et al.[8] where it was pointed out that the timescales accessible by the calculations are typically too short to allow for plastic deformation and that the elastic constants are dependent on the potential used for the calculations. For example, the elastic constants using the ME (Meyer-Entel) potential[8] predict an elastic curve that lies above the calculated curve shown in Fig. 6. In addition, the potential also affects the high-pressure Hugoniot where the deviation from the experimental Hugoniot was attributed to the "softness" of the potential upon compression. Based on the transition rate and the Hugoniot data obtained in the current work, it is expected that the dynamic response of shocked iron will qualitatively approach the MD simulations as the impact stress increases where the phase transition is overdriven and the material transforms at the limiting rate to the high-pressure Hugoniot.

VI. SUMMARY AND CONCLUSIONS

Plate impact experiments were performed to examine single crystal iron shocked along the [100] direction to impact stresses up to 20 GPa. The objectives of the current work were to obtain Hugoniot data for the α and ϵ phases of iron, to determine the transition stress for the single crystals, and the associated transition kinetics for the α-ϵ phase transition. These objectives were addressed by performing front surface impact and transmission experiments on single crystal and polycrystalline iron and using VISAR to obtain the particle velocity history at the iron/sapphire interface. These front-surface, plate-impact experiments were ideal for examining the pressure dependent kinetics of the phase transition of shocked iron.

For low velocity experiments, a single shock jump was observed followed by a release due to the free-surface located at the back of the iron impactor. As the projectile velocity increased, a transient wave profile was observed that consisted of a velocity spike followed by a relaxation to a peak steady state. The relaxation time was observed to decrease with pressure until the spike was undetectable for impact stresses greater than approximately 19-20 GPa. Analysis of the Hugoniot data revealed that the initial compression of the iron samples was consistent with stress states along the phase-I Hugoniot which was equivalent to the calculated mean stress curve. The Hugoniot equations for single crystal and polycrystal iron in the metastable region were determined by fitting the stress-particle velocity data to polynomial functions for both. The intersection of the two Hugoniots with the mean stress curve were taken as the transition stress for the α-ϵ phase transition. For single crystal iron, the phase transition stress was found to be 14.26 GPa; significantly greater than the polycrystal value of 12.8 GPa. The higher transition stress (as compared to polycrystal) is in agreement with the predictions from molecular dynamics simulations that describe

an orientation dependence of the transition stress. However, the MD calculations[8] do not capture the full complexity of shock response of iron including the transition kinetics as well as the Hugoniot states. This is due to the limitations on timescales in these calculations as well as limitations in the potential function used.

Direct measurements of the transition kinetics for polycrystal and single crystal iron shock compressed to stresses that span the elastic-plastic and α-ϵ phase transition have been obtained. The data reveal an orientation dependence of the transition stress coupled with a transition time that is nonlinearly dependent on the impact stress with a duration ranging from hundreds of ns near the transition stress to less than a nanosecond for impact stresses greater than 180 kbar. The data were compared to a previous analysis by Boettger[6] revealing significant difference in the transition rates (and functional form) for front-surface and transmission experiments. Work is underway to investigate this finding along with additional data for the [111] and [110] orientation of iron to provide additional insight into the mechanisms that govern the phase transition.

VII. ACKNOWLEDGMENTS

This work was conducted by Los Alamos National Laboratory operated by Los Alamos National Security, LCC for the U.S. Department of Energy's NNSA. Special thanks to B.H. Sencer for the initial sample preparation. Jim Esparza, Frank Abeyta, Mark Byers, and Chuck Owens are gratefully acknowledged for their help in target and projectile fabrication, gun setup, and shot execution. Thanks to F. Cherne for discussions related to MD calculations and thanks to K. Kadau for providing his calculated iron single crystal Hugoniot data for comparison with the data obtained in this work.

---

* Electronic address: bjjensen@lanl.gov
† Current Address: Naval Post Graduate School, Monterey, CA

[1] D. Bancroft, E. L. Peterson, and S. Minshall, J. Appl. Phys. **27(3)**, 291 (1956).
[2] J. C. Jamieson and A. W. Lawson, J. Appl. Phys. **33(3)**, 776 (1961).
[3] T. Takahashi and W. A. Basset, Science **145**, 483 (1964).
[4] L. M. Barker and R. E. Hollenbach, J. Appl. Phys. **45(11)**, 4872 (1974).
[5] D. J. Andrews, J. Phys. Chem. Solids **34**, 825 (1973).
[6] J. C. Boettger and D. Wallace, Phys. Rev. B **55**, 2840 (1997).
[7] L. R. Veeser, G. T. Gray III, et al., Shock compression of condensed matter pp. 73–76 (2000).
[8] K. Kadau, T. C. Germann, P. S. Lomdahl, and B. L. Holian, in *Shock compression of condensed matter*, edited by M. D. Furnish, N. N. Thadhani, and Y. Horie (American Institute of Physics, 2001), pp. 351–354.
[9] K. Kadau, T. C. Germann, P. S. Lomdahl, and B. L. Holian, Phys. Rev. B **72**, 064120 (2005).
[10] B.J. Jensen, P.A. Rigg, M.D. Knudson, et al., in *Shock compression of condensed matter*, edited by E. M. R. T. W. C. Furnish, M. D. (American Institute of Physics, 2006), pp. 232–234.
[11] D. H. Kalantar, E. A. Chandler, J. D. Colvin, R. Lee, B. A. Remington, S. V. Weber, A. Hauer, J. S. Wark, A. Loveridge, M. A. Meyers and G. Ravichandran, Rev. Sci. Ins. **70**, 629 (1999).
[12] B.J. Jensen and Y.M. Gupta, J. Appl. Phys. **104**, 013510 (2008).
[13] D. B. Hayes, J. Appl. Phys. **45**, 1208 (1974).
[14] L. M Barker and R. E. Hollenbach, J. Appl. Phys. **43**, 4669 (1972).
[15] W. F. Hemsing, Rev. Sci. Instrum **50**, 73 (1979).
[16] B.J. Jensen, D.B. Holtkamp, P.A. Rigg, D.H. Dolan, J. Appl. Phys. **101**, 013523 (2007).
[17] S.C. Jones and Y.M. Gupta, J. Appl. Phys. **88**, 5671 (2000).
[18] R. Feng and Y.M. Gupta, Tech. Rep., Shock Dynamics Center Internal Report 96-XX (1996).
[19] R. Setchell, J. Appl. Phys. **50**, 8186 (1979).
[20] S.C. Jones, M.C. Robinson, and Y.M. Gupta, J. Appl. Phys. **93**, 1023 (2003).
[21] G.E. Duvall and G.R. Fowles, in *High pressure physics and chemistry*, edited by R. Bradley (Academic Press, London, 1963).
[22] B. E. Powell and M. J. Skove, Phys. Rev. **174**, 977 (1965).
[23] Simmons, G. and Wang, H, *Single crystal elastic constants and calculated aggregate properties: A Handbook* (The MIT Press, Cambridge, Massachusetts, and London, England, 1971).
[24] R.N. Thurston, in *Physical Acoustics: Principles and Methods*, edited by W. Mason (Academic Press, New York, 1964), vol. 1A.
[25] J. M. Brown and R. G. McQueen, in *High Pressure Research in Geophysics*, edited by S. Akimoto and M. H. Manghnani (Center for Academic Publishing, Tokyo, 1982s), pp. 611–623.